Cancer Research

The Canonical Wnt Pathway Drives Macropinocytosis in Cancer

Gil Redelman-Sidi[1], Anna Binyamin[2], Isabella Gaeta[3], Wilhelm Palm[4], Craig B. Thompson[4], Paul B. Romesser[4], Scott W. Lowe[4], Mukta Bagul[5], John G. Doench[5], David E. Root[5], and Michael S. Glickman[1,2]

Abstract

Macropinocytosis has emerged as an important pathway of protein acquisition in cancer cells, particularly in tumors with activated Ras such as pancreatic and colon cancer. Macropinocytosis is also the route of entry of Bacillus Calmette-Guerin (BCG) and other microbial therapies of cancer. Despite this important role in tumor biology and therapy, the full mechanisms by which cancer cells can activate macropinocytosis remain incompletely defined. Using BCG uptake to assay macropinocytosis, we executed a genome-wide shRNA screen for macropinocytosis activators and identified Wnt pathway activation as a strong driver of macropinocytosis. Wnt-driven macropinocytosis was downstream of the β-catenin–dependent canonical Wnt pathway, was PAK1 dependent, and supported albumin-dependent growth in Ras-WT cells. In cells with activated Ras-dependent macropinocytosis, pharmacologic or genetic inhibition of Wnt signaling suppressed macropinocytosis. In a mouse model of Wnt-driven colonic hyperplasia via *APC* silencing, Wnt-activated macropinocytosis stimulated uptake of luminal microbiota, a process reversed by topical pharmacologic inhibition of macropinocytosis. Our findings indicate that Wnt pathway activation drives macropinocytosis in cancer, and its inhibition could provide a therapeutic vulnerability in Wnt-driven intestinal polyposis and cancers with Wnt activation.

Significance: The Wnt pathway drives macropinocytosis in cancer cells, thereby contributing to cancer growth in nutrient-deficient conditions and, in the context of colon cancer, to the early phases of oncogenesis. *Cancer Res; 78(16); 4658–70. ©2018 AACR.*

Introduction

Macropinocytosis is an endocytic process by which cells internalize extracellular fluid and its contents into large vesicles known as macropinosomes (1). Macropinocytosis is activated in certain specialized cell types, such as macrophages and immature dendritic cells, where it has roles in antigen capture and presentation (2). Activation of macropinocytosis is also a hallmark of some cancers, particularly tumors harboring activating mutations of Ras (3). Whereas the role of macropinocytosis in cancer was long unclear, it was recently demonstrated that Ras-transformed cancers use macropinocytosis as a route of nutrient uptake (3–5), suggesting that inhibition of macropinocytosis, thereby starving tumors of essential nutrients, is a potential therapeutic strategy for Ras-driven cancers.

Bacillus Calmette-Guerin (BCG), an attenuated strain of *Mycobacterium bovis*, is used to treat non–muscle-invasive bladder cancer (NMIBC; ref. 6). Bladder cancer cells are able to internalize BCG through macropinocytosis (7), a process dependent on activation of the Ras and *PI3K*–PTEN pathways upstream of the kinase PAK1 (7).

However, the relevance of macropinocytosis more broadly in cancer types without Ras or *PI3K* mutation is unclear, and the full complement of cellular mechanisms that may activate this pathway has not been examined. In an effort to identify additional pathways that mediate macropinocytic uptake in tumor cells, we performed a whole-genome shRNA screen for genes that suppress macropinocytosis, using BCG uptake by Ras wild-type bladder cancer cell lines as an assay for macropinocytic uptake (7). Here we describe this screen, which identified activation of the Wnt pathway as a driver of macropinocytosis, demonstrate that Wnt-driven macropinocytosis uses the same machinery as Ras-driven macropinocytosis, and demonstrate that Wnt pathway activation in colonic epithelium promotes macropinocytic translocation of bacteria into the colonic wall, indicating that activation of macropinocytosis due to APC inactivation may be the initiating event in intestinal polyposis.

Materials and Methods

Whole-genome gain-of-function screen of determinants of BCG uptake by bladder cancer cell lines

The screen design is shown in Fig. 1A. Three Ras wild-type cell lines (MGHU3, MGHU4, and VMCUB3) were used. The baseline ability of these cell lines to internalize a GFP-expressing BCG

[1]Division of Infectious Diseases, Memorial Sloan Kettering Cancer Center, New York, New York. [2]Immunology Program, Sloan Kettering Institute, Memorial Sloan Kettering Cancer Center, New York, New York. [3]Vanderbilt University School of Medicine, Nashville, Tennessee. [4]Cancer Biology and Genetics Program, Sloan Kettering Institute, Memorial Sloan Kettering Cancer Center, New York, New York. [5]Broad Institute of Massachusetts Institute of Technology and Harvard, Cambridge, Massachusetts.

Note: Supplementary data for this article are available at Cancer Research Online (http://cancerres.aacrjournals.org/).

Corresponding Author: Michael S. Glickman, Memorial Sloan Kettering Cancer Center, ZRC 1504 1275 York Ave, New York, NY 10065. Phone: 646-888-2368; Fax: 646-422-2124; E-mail: glickmam@mskcc.org

doi: 10.1158/0008-5472.CAN-17-3199

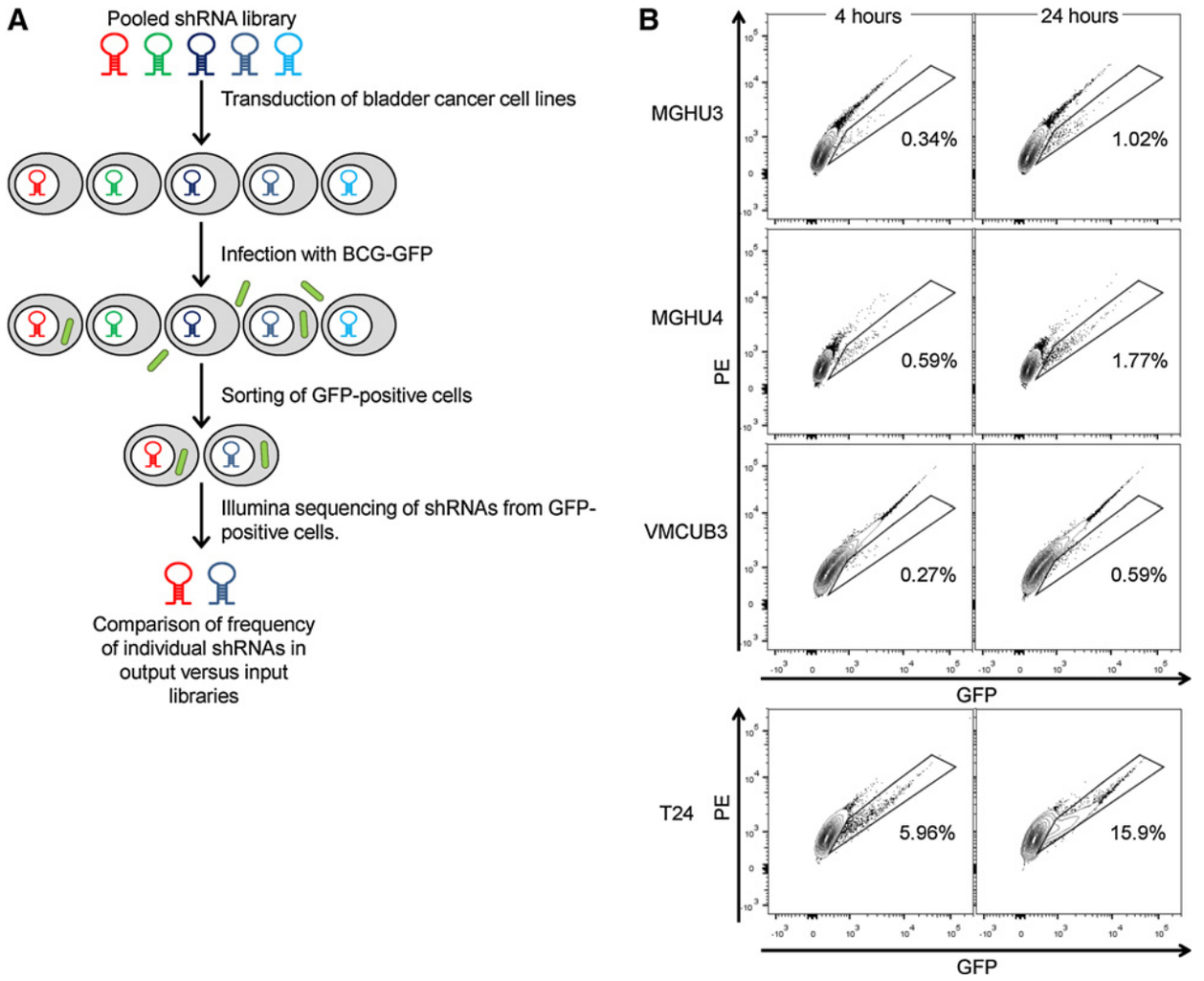

Figure 1.

A Whole-genome shRNA screen for inhibitors of macropinocytosis identifies inhibitors of Ras and Wnt pathways. **A,** Screen design. **B,** Top, flow cytometric quantitation of BCG-GFP uptake in the three cell lines used in the screen (MGHU3, MGHU4, and VMCUB3) at 4 hours or 24 hours after infection. Bottom, flow cytometric quantitation of BCG-GFP uptake at 4 hours or 24 hours after infection in the cell line T24, which harbors an *HRas* G12V activating mutation. *Y*-axis (PE) represents an empty channel used for gating purposes. *X*-axis represents GFP. Results are representative of three independent experiments.

strain (BCG-GFP) was determined by flow cytometry, as described previously (7). On the basis of these results, we anticipated a background infection rate of approximately 0.2%–0.5% for 4-hour infections and 1%–2% for 24-hour infections. We sorted 2.5 $\times$ 10^8 cells for 4-hour infection and 2.5 $\times$ 10^7 cells for a 24-hour infection, yielding an expected 5 $\times$ 10^5 background positive events, and representing each shRNA in the library with an average of 2,600 and 260 input cells, respectively.

Cell lines were grown in complete Eagle minimal essential medium (MEM) supplemented with 10% FBS, 1 mmol/L sodium pyruvate, 2 mmol/L L-glutamine, and 1:100 dilution of 100$\times$ MEM nonessential amino acids solution (NEAA, Thermo Fisher Scientific). Each cell line was transduced with the Broad Institute RNAi Consortium (TRC) shRNA library, consisting of approximately 95,000 pLK0.1 and pLK0.5-based shRNAs targeting nearly 17,000 genes (8). Transduction was performed in the presence of polybrene 4 μg/mL (Sigma-Aldrich). For each cell line, transduction was optimized to achieve a multiplicity of infection (MOI) of 0.3–0.5, corresponding to a <20% chance of cells expressing >1 shRNA.

Optimal concentration of puromycin for antibiotic selection was optimized for each cell line individually. After selection with puromycin (Sigma-Aldrich) for 4 days, cells were infected with BCG-GFP at a MOI of 10:1 for 4 hours or 24 hours and then washed three times in PBS followed by three washes with complete MEM containing penicillin–streptomycin (Invitrogen) to remove extracellular BCG. Cells were detached from plates using trypsin. FACS was used to sort GFP-positive (BCG-infected) cells. For each cell line, a non-BCG-GFP–infected control was used to determine the sorting gate. Representative flow plots and gates of the cell lines used in the screen and infected with BCG-GFP are shown in Fig. 1B.

Genomic DNA was extracted from the input shRNA library and from the sorted cells using QIAamp DNA blood kit (Qiagen). A two-step PCR was used to amplify the shRNA sequence from the genomic DNA of transduced cells, as described previously (8).

Positive hits were defined as genes for which at least 3 shRNAs (in the same replicate or in different replicates) were represented more than 4-fold in the sorted population of cells compared with the input pool of the shRNA library.

Pathway analysis of hits was performed using Molecular Signatures Database v6.0 (available at http://software.broadinstitute.org/gsea/msigdb/index.jsp; ref. 9).

Cell lines

The bladder cancer cell lines T24, UMUC3, 5637, MGHU3, MGHU4, and VMCUB3 were a gift from Dr. Dan Theodorescu (University of Colorado, Denver, Denver, CO) and were authenticated through mass spectrometry–based DNA fingerprinting, as described previously (10). A549 lung cancer cell line, Panc1 pancreatic cancer cell line, and SW1417 colon cancer cell line were purchased from ATCC and authenticated by the supplier by short tandem repeat profiling. Bladder cancer cell lines and SW1417 were grown in MEM. A549 and Panc1 were grown in DMEM. Media were supplemented with 10% FBS, 1 mmol/L sodium pyruvate, 2 mmol/L L-glutamine, and NEAA. Cells were cultured at 37°C in a humidified atmosphere of 5% CO_2 in air. All cell lines used were confirmed to be negative for *Mycoplasma* by annual testing using MycoAlertTMPlus (Lonza). Last date of mycoplasma testing was January 17, 2018.

BCG-GFP

BCG-GFP was created as described previously (7). BCG was grown at 37°C in Middlebrook 7H9 media supplemented with 10% albumin/dextrose/saline, 0.5% glycerol, and 0.05% Tween 80, and in the presence of 20 μg/mL kanamycin. To create tittered stocks for infection, BCG-GFP was grown to mid-log phase (OD600 0.4–0.6), washed twice in PBS with 0.05% Tween 80, resuspended in PBS with 25% glycerol, and stored at −80°C. To measure final bacterial titer, an aliquot was thawed, and serial dilutions were cultured on 7H10 agar media in the presence of 20 μg/mL kanamycin, and the bacterial titer determined by counting kanamycin-resistant colonies after 3 weeks of incubation.

BCG infection

Bladder cancer cells were plated a day prior to infection in antibiotic-free media to reach 50%–80% confluence on the day of infection. BCG was thawed, diluted in antibiotic-free media to achieve a multiplicity of infection (MOI) of 10:1, and added to the cells. After an incubation of 4 hours at 37°C, the cells were washed three times with PBS, three times with media containing 1% penicillin–streptomycin, rewashed with PBS, detached using trypsin, and resuspended in PBS for analysis by flow cytometry.

Flow cytometry

Cell suspensions were analyzed on an LSR II flow cytometer (BD Biosciences), using the FACS DiVa software (BD Biosciences) according to manufacturer's instructions. Statistical analysis was performed with the FlowJo software package (Tree Star). GFP was detected on the FITC channel using a 488 nm laser.

Pharmacologic inhibitors

For BCG infection, cells were pretreated with the inhibitors at the specified concentrations for 1 hour at 37°C. The media were then aspirated and replaced with media containing the inhibitor at the specified concentration plus BCG at an MOI of 10:1 for 4 hours at 37°C. For experiments involving measurement of dextran uptake, cells were pretreated with inhibitors at the specified concentrations for 4 hours prior to addition of dextran. In all experiments utilizing chemical inhibitors, the highest concentration of DMSO was used as vehicle control. Pharmacologic inhibitors used in this study are listed in the Supplementary Methods.

Plasmids and transfections

PLK0.1-based shRNA constructs for knockdown of KREMEN1, APC, and AXIN1 and miR30-based constructs for knockdown of DKK1 were constructed by the Memorial Sloan Kettering RNAi & Gene Editing core facility. pLKO.1-puro nontarget shRNA control (SHC016, SIGMA) was used as nontargeting control.

AXIN1 cDNA was purchased from MyBioSource and was cloned into pQCXIP-IRES-puro using the *Eco*RI and *Not*I restriction sites. pQCXIN-PAK1(L107F) and pQCXIP-KRAS(G12D) were constructed as described previously (7).

Lentivirus for shRNA knockdown of KREMEN1, AXIN1, and APC was made by cotransfecting the respective plasmids with Mission Lentiviral Packaging Mix (Sigma) into 293T cells using Lipofectamine 2000 (Invitrogen) as per the manufacturer's instructions. Lentiviruses for expression of pQCXIP-empty, pQCXIN-empty, pQCXIP-AXIN1, pQCXIP-KRAS(G12D), E (beta)P, and pQCXIN-PAK1(L107F) were made by cotransfecting the respective constructs with the packaging plasmids VSV-G and pCPG into 293T cells using Lipofectamine 2000. A day prior to infection with lentivirus, cell lines were plated in 6-well plates and allowed to attach overnight. On the day of infection media was replaced with supernatant from 293T plates, and polybrene 8 μg/mL (Sigma) was added. Plates were spun at 1,100 × *g* for 30 minutes. The media was replaced with fresh antibiotic-free media, and the plates were allowed to incubate overnight. The following day, cells containing the lentiviral insert were selected using puromycin (Invitrogen) or G418 (Sigma) for 4 days. Cells that had not been infected with lentivirus were used as control for selection.

shRNA sequences are listed in the Supplementary Methods.

FISH

FISH was conducted as described previously (11). Briefly, tissue sections were deparaffinized twice with xylene (10 minutes each) and rehydrated by successive 10-minute washes with 95% ethanol, 90% ethanol, and water. Bacteria were stained using a fluorescent universal bacterial probe EUB338 (purchased from IDT) directed against the 16S rRNA gene (11). Sequence of the EUB338 probe is as follows: 5′[Cy3]/GCTGCCTCCCGTAGGAGT/[Cy3]3′. Probe was diluted to 10 ng/μL in 0.9 mol/L NaCl, 20 mmol/L Tris-HCl at pH 7.2, and 0.1% SDS. Slides containing the probe were covered with Frame-Seal hybridization chambers (Thermo Fisher Scientific). After 3 hours of incubation at 50°C, sections were washed twice in 0.9 mol/L NaCl, 20 mmol/L Tris-HCl at pH 7.2 for 10 minutes and counterstained with DAPI for nuclear staining.

Antibodies

The following antibodies were used for Western blot analysis: β-actin (Cell Signaling Technology #3700), AXIN1 (Cell Signaling Technology #2087), PAK1 (Cell Signaling Technology #2602), human APC (Abcam ab58), mouse APC (Abcam ab15270), DKK1 (R&D Systems AF1096), and KREMEN1 (R&D Systems MAB2127).

Measurement of the macropinocytic index

The macropinocytic index was measured as described previously (12). Briefly, cells were plated in Nunc Lab-Tek II chamber slides and allowed to attach for 18–24 hours. Lysine-fixable Texas Red–labeled dextran molecular weight 70,000 (Thermo-Fisher Scientific #D1864) was diluted in media to a final concentration of 1 mg/mL and incubated with cells at 37°C for 30 minutes. After washing 5 times with ice-cold PBS, cells were then fixed in 4% paraformaldehyde for 15 minutes at room temperature and washed twice with PBS. DAPI (Thermo Fisher Scientific #D1306) was applied to each well at a concentration of 0.5 μg/mL for 15 minutes, followed by two PBS washes. The slides were mounted with SlowFade Diamond Antifade Mountant (Thermo Fisher Scientific #S36972).

Images were acquired on a Zeiss Axiovert inverted 200M widefield microscope using a 63× oil objective. Images of 15–20 random fields, each containing 10 to 30 cells, were acquired for each sample. Images were analyzed using ImageJ software (http://imagej.nih.gov/ij/) as described previously (12).

Albumin-dependent growth assay

To measure albumin-dependent growth, 2×10^5 cells per well were plated in in a 6-well plate in complete MEM. After 16 hours media was removed and the cells washed twice in PBS. Cells were placed in MEM lacking the essential amino acid leucine and supplemented with 10% dialyzed FBS, 2 mmol/L L-glutamine and NEAA, with or without the addition of 6% BSA (Sigma; ref. 5). The media were replaced daily. After 72 hours of growth in media lacking leucine, cells were washed with PBS, detached using trypsin, and counted using a hemocytometer.

Wnt luciferase reporter assay

Cells were stably transduced with the 7TFC Wnt reporter, a lentiviral vector expressing firefly luciferase under the control of a Wnt-dependent TCF promoter (13). The same number of cells was used for each condition. Luciferase activity in the lysates was measured using the Promega Luciferase Assay system according to the manufacturer's instructions.

Animals

Production of mice and all treatments described were approved by the Institutional Animal Care and Use Committee at Memorial Sloan Kettering Cancer Center (New York, NY). Doxycycline was administered via food pellets (625 mg/kg; Harlan Teklad).

Primers used for genotyping are listed in the Supplementary Methods.

Dextran uptake in mouse colons

shApc and control mice were treated with oral doxycycline for 8 days. Mice were anesthetized in an isoflurane chamber and a 3.5 French polyurethane catheter (Access Technologies catalog# CNC-3.5P-6″/LSA22) was inserted through the anus to a distance of 1 inch. Texas Red fluorescent dextran molecular weight 70,000 (Invitrogen catalog# D1864) was diluted in PBS to a final concentration of 1mg/mL, and a volume of 200μl was instilled into the colon for 45 minutes. In experiments using intracolonic ethylisopropyl amiloride (EIPA), EIPA (100 μmol/L) or DMSO (0.1%) was diluted in PBS. A volume of 200 μl was instilled into the colon for 45 minutes. The catheter was removed, and a new catheter inserted, through which, 200 μl of Texas Red dextran 1mg/mL containing EIPA (100 μmol/L) or DMSO (0.1%) was instilled and kept in the colon for an additional 45 minutes.

Mice were euthanized in a CO2 chamber and the colons were removed from the level of the rectum to the splenic flexure. The colons were fixed in 4% PFA overnight and were paraffin-embedded. Slides were submitted for immunofluorescence.

Western blot analysis of mouse colons

shApc and control mice were treated with oral doxycycline for 8 days. Mice were euthanized and their colons were removed. Colons were cut longitudinally and washed in Hank's Balanced Salt Solution (HBSS). Colons were incubated in 2 mmol/L EDTA in HBSS at 37°C for 15 minutes and agitated vigorously. The supernatant containing epithelial fraction was collected by centrifugation and resuspended in Western blot lysis buffer.

Immunofluorescence

Immunofluorescent staining was performed at the Molecular Cytology Core Facility of Memorial Sloan Kettering Cancer Center using a Discovery XT processor (Ventana Medical Systems). Tissue sections were deparaffinized with EZPrep buffer (Ventana Medical Systems), and antigen retrieval was performed with CC1 buffer (Ventana Medical Systems). Sections were blocked for 30 minutes with Background Buster solution (Innovex), followed by avidin–biotin blocking for 8 minutes (Ventana Medical Systems). Multiplex immunofluorescent staining was performed as described previously (14).

Sections were incubated with MUC2 antibody (Santa Cruz Biotechnology, #sc15334, 1 μg/mL) for 5 hours, followed by 1-hour incubation with biotinylated goat anti-rabbit IgG (Vector Laboratories, #PK6101) at 1:200 dilution. The detection was performed with Streptavidin-HRP D (part of DABMap kit, Ventana Medical Systems), followed by incubation with Tyramide Alexa Fluor 488 (Invitrogen, #B40953) prepared according to the manufacturer's instruction with predetermined dilutions. Next, sections were incubated with anti-CK8/18 (Abcam #ab53280, 0.12 μg/mL) for 5 hours, followed by 60-minute incubation with biotinylated goat anti- rabbit IgG (Vector Laboratories, catalog no. PK6101) at 1:200 dilution. Detection was performed with Streptavidin-HRP D, followed by incubation with Tyramide Alexa 647 (Invitrogen #B40958) prepared according to the manufacturer's instruction with predetermined dilutions. Staining slides were the counterstained with DAPI (Sigma Aldrich # D9542, 5 μg/mL) for 10 minutes. Coverslips were mounted with Mowiol.

Images were obtained on a Zeiss Axio2Imaging upright widefield microscope using a 40× objective. Images of 20–30 fields were acquired for each specimen. Images were analyzed using ImageJ software.

Statistical analysis

The group means for different treatments were compared, as indicated, by ANOVA with Bonferroni multiple comparisons test, or by a two-sided Student *t* test analysis. A $P \leq 0.05$ was considered significant.

Results

A whole-genome gain-of-function screen for activators of macropinocytosis

A whole-genome shRNA screen for hairpins that enhance BCG uptake was conducted. The screen design is described in

detail in the Materials and Methods section and is outlined in Fig. 1A. Three cell lines were used, all of which express wild-type Ras and do not engulf BCG by macropinocytosis. Representative flow plots showing baseline infection rates for these cell lines at the two time points used in the screen are shown in Fig. 1B. T24, a HRAS-G12V-expressing cell line previously characterized to have an activated macropinocytosis (3), is shown for comparison.

A total of 570 genes fulfilled our definition of a positive hit (Table S1). We identified multiple genes involved in vesicular transport, phosphatidylinositol metabolism, and the Ras pathway. Although many of these genes have not been extensively characterized, the identification of a negative regulator of Ras, the tumor suppressor *NF1*, validates that the screen can identify activators of macropinocytosis. To determine which pathways were overrepresented in the screen hits, we performed pathway analysis (Supplementary Table S2). Among pathways significantly enriched was the Wnt signaling pathway. Five of the 7 Wnt genes detected as macropinocytic activators were negative regulators of the Wnt signaling pathway. These included *DKK2*, *KREMEN1*, *NKD1*, *SMAD4*, and *MAPK9* (15–20).

Activation of the canonical Wnt pathway stimulates macropinocytic BCG uptake

Signaling through the Wnt pathway commences with binding of a soluble Wnt ligand to its receptor LRP6. Activation of the pathway is subject to negative regulation at multiple points in the pathway, including through internalization of the receptor at the cell surface and through proteolytic control of the CTNNB1 (β-catenin) transcription factor in the destruction complex (21). To ascertain whether activation of the Wnt pathway stimulates macropinocytic uptake of BCG, we first focused on KREMEN1 and DKK1. Binding of the secreted protein DICKKOPF1 (DKK1) to its receptor, KREMEN1, results in endocytic removal of the Wnt receptor LRP6 from the plasma membrane, thereby blocking signaling via the canonical Wnt pathway (16). Depletion of KREMEN1 protein by three different KREMEN1 shRNAs stimulated BCG uptake in three different Ras wild-type bladder tumor cell lines (Fig. 2A: Supplementary Fig. S1A and S1B). Similarly, knockdown of DKK1 by four distinct shRNAs activated macropinocytosis in all three cell lines tested, although to varying degrees (Fig. 2B; Supplementary Fig. S1C and S1D).

Our prior work determined that the mechanism of BCG uptake into bladder cells is via a Pak1-dependent macropinocytosis pathway in cells harboring activating mutations of Ras (7). To determine whether Wnt activated uptake uses the same machinery, we tested the effect of chemical inhibition with either EIPA, a Na–H pump inhibitor that inhibits macropinocytosis (22), or IPA-3, an inhibitor of PAK1 (23) on a Ras wild-type bladder cancer cell line transduced with either DKK1 or KREMEN1 shRNA. We found that both EIPA and IPA-3 completely abrogated the increase in BCG uptake engendered by DKK1 or KREMEN1 knockdown (Fig. 2C), confirming that this uptake is via PAK1-dependent macropinocytosis. Neither EIPA nor IPA-3 resulted in cell death under the conditions used here (Supplementary Fig. S1E).

The Wnt pathway is a branched pathway with three arms. In the canonical Wnt/β-catenin branch, binding of a Wnt ligand to the Frizzled-LRP5/6 receptor complex results in dissociation of the β-catenin destruction complex (composed of APC, AXIN, and GSK3), allowing the accumulation and translocation of β-catenin into the nucleus and activation of its target genes (24). The two main noncanonical pathways are the planar cell polarity (PCP) pathway and the Wnt/Ca^{2+} pathway, both of which are independent of the β-catenin destruction complex (24). Signaling through DKK1 and KREMEN1 primarily affects the canonical Wnt pathway (25), but may have some Wnt-independent functions (26). To test whether the increase of macropinocytic BCG uptake engendered by KREMEN1 or DKK1 knockdown is dependent on Wnt activation of nuclear β-catenin, we tested the effect of ICG001, an inhibitor of the interaction between β-catenin and cyclic AMP response element-binding protein (27), on BCG uptake in a Ras wild-type cell line transduced with nontargeting shRNA, KREMEN1 shRNA or DKK1 shRNA. We found that the increase in BCG uptake engendered by KREMEN1 or DKK1 knockdown was completely abrogated by treatment with ICG001, indicating that the effect of KREMEN1 or DKK1 knockdown is mediated through the canonical Wnt pathway and β-catenin–driven transcription (Fig. 2D).

To further test whether the stimulation of macropinocytosis observed with DKK1/KREMEN1 loss proceeds through the canonical Wnt pathway we focused on adenomatous polyposis coli (APC), a vital component of the β-catenin destruction complex and a key tumor suppressor gene, most notably in colon cancer (28). To test the role of APC in BCG uptake, we transduced Ras wild-type cells with APC shRNA and tested the effect on uptake of BCG-GFP. Loss of APC resulted in a 2- to 5-fold increase in BCG uptake that paralleled the expected increase in Wnt pathway activation in three different Ras WT bladder tumor cell lines, as measured by a luciferase reporter (Fig. 2E and F; Supplementary Fig. S1F–S1H). Taken together, these data demonstrate that the canonical Wnt pathway is sufficient to activate the Pak1-dependent macropinocytosis pathway in Ras wild-type cancer cells.

Activation of the Wnt pathway is sufficient to support albumin-dependent cell growth

To further characterize Wnt-driven macropinocytosis, we used a quantitative macropinocytosis assay that measures uptake of fluorescent high molecular weight dextran by fluorescence microscopy to yield the macropinocytic index (3, 12). We validated the assay by demonstrating inhibition of uptake of fluorescent dextran with EIPA treatment (Supplementary Fig. S2A and S2B).

Treatment with recombinant Wnt3A protein (rWnt3A), which activates the canonical Wnt pathway (Fig. 3A), significantly increased the macropinocytic index (Fig. 3B and C; Supplementary Fig. S3). Similarly, expression of E(beta)P, a constitutively activated form of β-catenin (13), significantly increased the macropinocytic index (Fig. 3D–F; Supplementary Fig. S4). Moreover, the increase in dextran uptake engendered by E(beta)P was abrogated by chemical inhibition with IPA-3, suggesting that it was dependent on PAK1 (Fig. 3G). Next, we tested the effect of DKK1 knockdown on dextran uptake and found that knockdown of DKK1 resulted in a 33% to 325% increase in the uptake of fluorescent dextran by all cell lines tested (Fig. 3H; Supplementary Fig. S5A and S5B). Interestingly, knockdown of DKK3 was previously shown to induce cell death due to activation of macropinocytosis in the Ras-mutant cell line T24 (29). Knockdown of DKK1, however, did not cause cell death to the cell lines used in our assays (Supplementary Fig. S5C). AXIN1 is a member of the β-catenin destruction complex that negatively regulates the Wnt

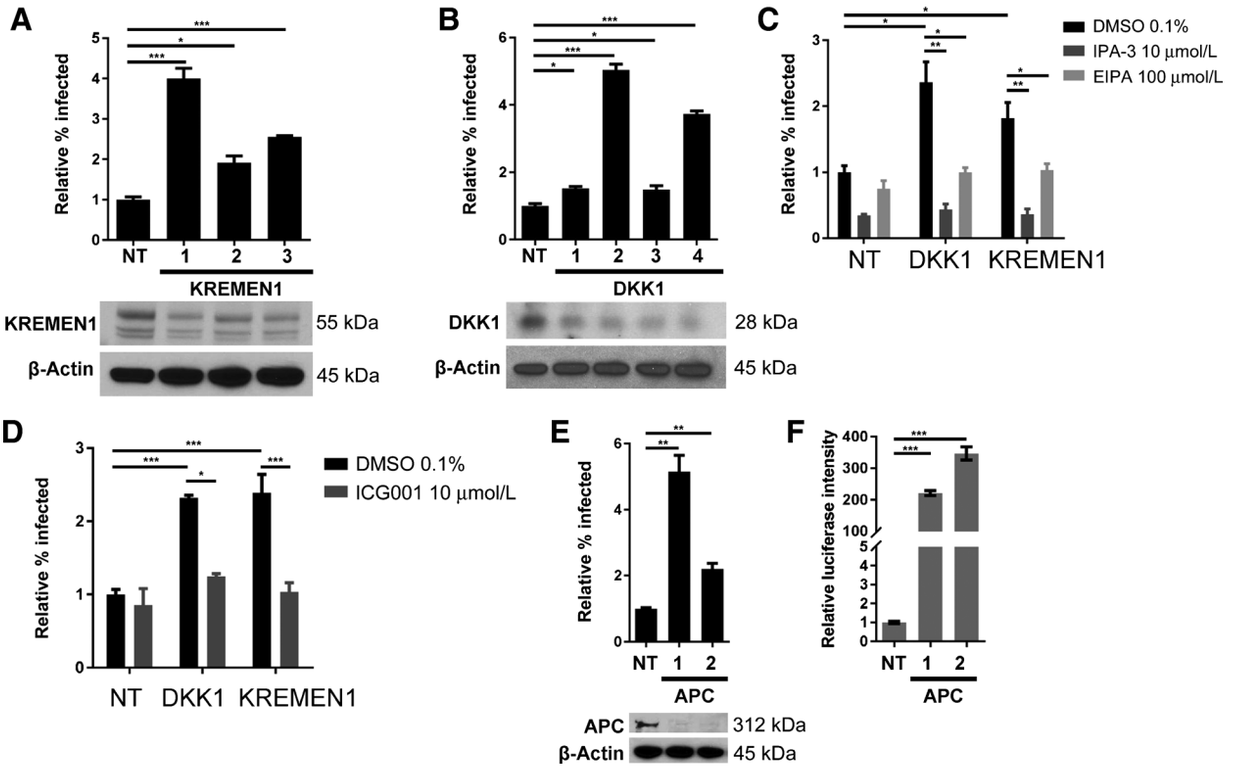

Figure 2.

Activation of the canonical Wnt pathway stimulates macropinocytic BCG uptake **A,** The bladder cancer cell line MGHU4 was transduced with nontargeting (NT) or three distinct KREMEN1 shRNAs (1–3) and incubated with BCG-GFP for 4 hours. Uptake of BCG-GFP was measured by flow cytometry. Knockdown of KREMEN1 for each shRNA is shown by Western blot analysis, with β-actin as a loading control. The data correspond to the mean of three independent experiments ± SEM. **B,** MGHU4 cells were transduced with nontargeting or four distinct DKK1 shRNAs and incubated with BCG-GFP for 4 hours. Uptake of BCG-GFP was measured by flow cytometry. Knockdown of DKK1 for each shRNA is shown by Western blot analysis, with β-actin as a loading control. The data correspond to the mean of three independent experiments ± SEM. **C,** MGHU4 cells were transduced with nontargeting shRNA, DKK1 shRNA#2, or KREMEN1 shRNA#3 and incubated with BCG-GFP for 4 hours in the presence of IPA-3 (Pak1 inhibitor), EIPA (macropinocytosis inhibitor), or DMSO (vehicle control). Uptake of BCG-GFP was measured by flow cytometry. The data corresponds to the mean of three independent experiments ± SEM. **D,** MGHU4 cells were transduced with nontargeting shRNA, DKK1 shRNA#2, or KREMEN1 shRNA#3 and incubated with BCG-GFP for 4 hours in the presence of ICG001 or DMSO (vehicle control). Uptake of BCG-GFP was measured by flow cytometry. The data corresponds to the mean of three independent experiments ± SEM. **E,** MGHU4 cells were transduced with nontargeting or two different APC shRNAs and incubated with BCG-GFP for 4 hours. Uptake of BCG-GFP was measured by flow cytometry. Knockdown of APC for each shRNA is shown by Western blot analysis, with β-actin as a loading control. The data corresponds to the mean of three independent experiments ± SEM. **F,** MGHU4 cells stably expressing the Wnt reporter construct 7TFC were transduced with nontargeting or APC shRNA. Luciferase expression in cell lysates was measured by luminometry. The data corresponds to the mean of three independent experiments ± SEM. *P* values derived by ANOVA with Bonferroni correction, $P < 0.05$; **, $P < 0.005$; ***, $P < 0.0005$.

pathway (30). Accordingly, AXIN1 knockdown increased uptake of dextran by the cell lines tested by 46% to 710% (Fig. 3I and J; Supplementary Fig. S5D–S5G). EIPA abrogated the dextran uptake stimulated by AXIN1 knockdown, confirming it is through the macropinocytosis pathway (Fig. 3K).

Cancers harboring activating mutations of Ras utilize macropinocytosis for uptake of extracellular fluid proteins, such as albumin. Albumin uptake by macropinocytosis is the first step in a complex metabolic rewiring that can allow cancer cells to proliferate using extracellular protein as a source of essential amino acids (3–5, 31). To determine whether the increase in macropinocytosis resulting from Wnt pathway activation is sufficient to support albumin-dependent cell growth, we made use of a recently described assay in which cells are grown in medium lacking leucine, an essential amino acid, in the absence or presence of BSA (5). We found that treatment with rWnt3A, expression of E(beta)P or knockdown of AXIN1 supported cell growth in leucine-free media in the presence of BSA (Fig. 3L–N; Supplementary Fig. S5H). To determine whether the magnitude of macropinocytic activation conferred by WNT activation is comparable with that observed in cells carrying an activated Ras allele, we directly compared T24 cells with three different Ras WT cells with AXIN1 knockdown. We observed that the absolute macropinocytic index in WNT-activated cells was higher than in T24, confirming that WNT activation alone supports robust macropinocytosis (Supplementary Fig. S5I).

Taken together, these experiments indicate that activation of the canonical Wnt pathway via nuclear β-catenin is sufficient to drive macropinocytosis in cancer cells and can support tumor cell growth by uptake of exogenous protein as a source of essential amino acids.

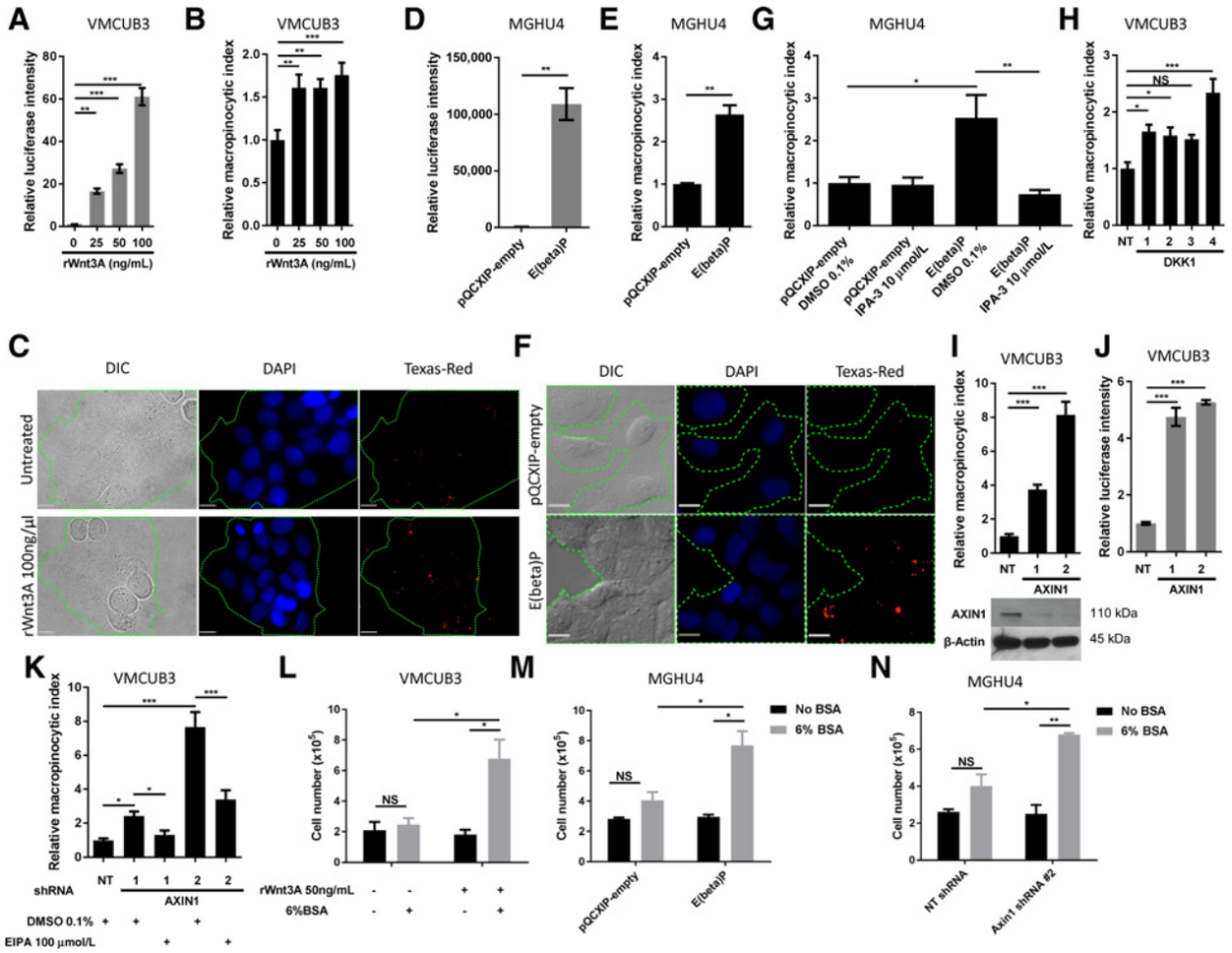

Figure 3.

Activation of the Wnt pathway is sufficient to support albumin-dependent cell growth **A,** VMCUB3 cells were transduced with the Wnt reporter construct 7TFC and were then treated with indicated concentrations of rWnt3A for 4 hours. Lysates were assayed by luminometry to determine relative luciferase activity. The data correspond to the mean of three independent experiments ± SEM. **B,** VMCUB3 cells were treated with indicated concentrations of rWnt3A for 4 hours and Texas Red dextran was added for 30 minutes in presence of rWnt3A. Cells were washed and fixed. Macropinocytic index was measured by analysis of microscopy images. The data correspond to the mean of three independent experiments ± SEM. **C,** Representative microscopic images of **B**. Scale bars, 18 μm. Cell borders are outlined in green. **D,** MGHU4 cells were transduced with the Wnt reporter construct 7TFC and were transduced with E(beta)P or with an empty construct. Lysates were assayed by luminometry to determine relative luciferase activity. The data correspond to the mean of three independent experiments ± SEM. **E,** MGHU4 cells were transduced with E(beta)P or with an empty construct. Texas Red dextran was added for 30 minutes. Cells were washed and fixed. Macropinocytic index was measured by analysis of microscopy images. The data correspond to the mean of three independent experiments ± SEM. **F,** Representative microscopic images of **E**. Scale bars, 12 μm. Cell borders are outlined in green. **G,** MGHU4 cells were transduced with E(beta)P or with an empty construct and treated with IPA-3 or DMSO for 4 hours, followed by 30 minutes with Texas Red dextran in the presence of IPA-3 or DMSO. Macropinocytic index was measured. The data correspond to the mean of three independent experiments ± SEM. **H,** VMCUB3 cells were transduced with nontargeting (NT) or DKK1 shRNA. Texas Red dextran was added for 30 minutes and the macropinocytic index was measured. The data correspond to the mean of three independent experiments ± SEM. **I,** VMCUB3 cells were transduced with nontargeting or AXIN1 shRNA. Texas Red dextran was added for 30 minutes and the macropinocytic index was measured. Knockdown of Axin1 was confirmed by Western blot analysis, with β-actin as a loading control. The data correspond to the mean of three independent experiments ± SEM. **J,** VMCUB3 cells transduced with the Wnt reported construct 7TFC were transduced with a nontargeting or AXIN1 shRNA. Lysates were assayed by luminometry to determine relative luciferase activity. The data correspond to the mean of three independent experiments ± SEM. **K,** VMCUB3 cells were transduced with NT or AXIN1 and treated with EIPA or DMSO for 4 hours, followed by 30 minutes with Texas Red dextran in the presence of EIPA or DMSO. The macropinocytic index was measured. The data correspond to the mean of three independent experiments ± SEM. **L,** VMCUB3 cells were grown for 72 hours in leucine-free growth medium in the presence or absence of 6% BSA, with or without addition of rWnt3A. After 72 hours, cells were counted. The data correspond to the mean of three independent experiments ± SEM. **M,** MGHU4 cells were transduced with E(beta)P or with an empty construct and grown for 72 hours in leucine-free growth medium in the presence or absence of 6% BSA. After 72 hours, cells were counted. The data correspond to the mean of three independent experiments ± SEM. **N,** MGHU4 cells were transduced with nontargeting or with Axin1 shRNA#2 and grown for 72 hours in leucine-free growth medium in the presence or absence of 6% BSA. After 72 hours, cells were counted. The data correspond to the mean of three independent experiments ± SEM. *P* values for **A**, **B**, **G**–**N** derived by ANOVA with Bonferroni's correction. *P* values for **D** and **E** derived by Student *t* test. rWnt3A, recombinant Wnt3A; EIPA, ethyl-isopropyl amiloride; DMSO, dimethyl sulfoxide; NS, nonsignificant.

Wnt pathway activation is an essential cofactor in Ras-driven macropinocytosis

The data presented above demonstrated that activation of the Wnt pathway is sufficient to drive macropinocytosis and support albumin dependent cell growth. To determine the correlation between BCG uptake by macropinocytosis and Wnt pathway activation across a range of Ras WT and Ras mutant cells lines, we transduced a panel of bladder cancer cell lines in which BCG uptake had been previously determined (7) with the β-catenin transcriptional reporter construct and measured levels of Wnt activation. We found that T24, UMUC3, 5637 and SW1710 cells, all of which are permissive for BCG uptake by macropinocytosis, had significantly higher basal levels of Wnt activation than MGHU3, MGHU4 and VMCUB3, which are non-permissive for BCG uptake by macropinocytosis (7), supporting a correlation between macropinocytosis and Wnt pathway activation (Fig. 4A).

Next, we explored the effect of inhibition of the canonical Wnt pathway on cells with activated macropinocytosis by exploiting a panel of small-molecule inhibitors that included BML286, an inhibitor of disheveled (32), IWR1, a tankyrase inhibitor (33), and ICG001. In nearly all cases, the three inhibitors decreased macropinocytic uptake of BCG (Fig. 4B, Supplementary Fig. S6A, S6B, S6C). ICG001, which of the three inhibitors targets the most downstream part of the canonical Wnt pathway, had the most profound effect on BCG uptake in the cell lines tested. None of the inhibitors caused significant cell death under these conditions (Supplementary Fig. S6D).

To ask whether Wnt pathway activation is broadly relevant to macropinocytosis in cell lines from diverse tumor types harboring activating mutations of Ras, we used the quantitative macropinocytosis assay in Ras mutant cells of pancreatic, lung, colon, and bladder origin. All of these cell lines, which display activated macropinocytic index, showed dose-dependent inhibition of dextran uptake by WNT pathway inhibition by ICG001 (Fig. 4C–E, Supplementary Fig. S7, S8A). ICG001 also inhibited dextran uptake in a Ras-wild-type cell line transduced with a cDNA encoding *KRAS* G12D, a mutant form of Ras (Fig. 4F). Moreover, the effect of ICG001 was abrogated by expression of a cDNA encoding *PAK1*(L107F), a constitutively activated form of PAK1 (Fig. 4G). These results indicate that inhibition of the Wnt pathway by ICG001 abrogates Ras-driven macropinocytosis across diverse Ras mutant tumor types in a Pak1 dependent manner.

As small-molecule inhibitors such as ICG001 may have off-target effects, we next sought to genetically inhibit Wnt signaling using ectopic gene expression. We overexpressed AXIN1 in our panel of cell lines harboring activating Ras mutations, and tested the effect on the macropinocytic index. AXIN1 overexpression inhibited dextran uptake by macropinocytosis by the bladder cancer cell lines T24 and UMUC3 and by the lung cancer cell line A549, and abrogated the albumin dependent cell growth in leucine free media (Fig. 4H–J, Supplementary Fig. S8B-D, S9).

Finally, to determine whether the inhibition of macropinocytosis by AXIN1 overexpression is mediated through PAK1, we transduced cells harboring AXIN1 overexpression with a cDNA encoding *PAK1*(L107F). *PAK1*(L107F) rescued the macropinocytic defect engendered by AXIN1 overexpression, indicating that the effect of AXIN1 on macropinocytosis was upstream of PAK1 (Fig. 4K). Interestingly, overexpression of AXIN1 increased PAK1 protein, suggesting that AXIN1 may stabilize PAK1 protein or affect *PAK1* gene expression in a yet unknown fashion.

Altogether, these findings indicate that inhibition of the canonical Wnt pathway in cancer cells harboring activating Ras mutations reduces macropinocytosis in a PAK1 dependent manner and impairs the ability of these cells to utilize protein as a source of essential amino acids.

Wnt pathway activation drives macropinocytic uptake of colonic luminal microbiota

Activation of the Wnt pathway, most commonly due to null mutation of APC, is a hallmark of early colorectal cancer and the genetic disorder familial adenomatous polyposis, and is a key step in colorectal oncogenesis (34, 35). Another important determinant of colorectal oncogenesis is the intestinal microbiome. In mouse models of colonic Wnt pathway activation, significantly fewer tumors are seen in germ-free or antibiotic-treated mice, and it has been suggested that loss of the integrity of the epithelial barrier in colon tumors results in increased translocation of bacteria and their products from the lumen into wall of the colon, giving rise to an inflammatory response that promotes oncogenesis (36–38). However, the specific mechanisms that control this barrier defect are unknown. We hypothesized that the activation of macropinocytosis we have shown with Wnt pathway activation would, when present in the colonic epithelium, stimulate macropinocytic uptake of bacteria and their products into the colonic wall.

To test this hypothesis, we utilized the shApc mouse model (39, 40). shApc mice possess in the Rosa26 locus a reverse tet-transactivator (rtTA), which drives expression of a tetracycline responsive element (TRE)-regulated miR30-based APC shRNA (39, 40). Treatment of shApc mice with doxycycline causes robust depletion of APC and activation of Wnt-dependent transcription (40), providing a model to test the effect of acute Wnt pathway activation on macropinocytosis *in vivo*. We treated mice with doxycycline for 8 days, a time point at which the shApc mice have robust activation of the Wnt pathway in their colon epithelium but are not yet ill-appearing or lethargic (40). As controls, we used doxycycline-treated Rosa26-rtTA mice, which possess the reverse tet-transactivator but lack the APC shRNA.

To quantitatively assess the effect of Wnt activation on colonic macropinocytosis, we adapted the fluorescent-dextran–based macropinocytosis assay to measure macropinocytic uptake of dextran by the colonic epithelium. shApc and control mice received intracolonic instillation of Texas Red fluorescent high molecular weight dextran. After incubation, the colons were removed and sections were stained by immunofluorescence for cytokeratins 8/18 to delineate the colonic epithelial cells. Dextran uptake was quantitated by measuring the area of Texas Red fluorescence as a fraction of total area positive for cytokeratin 8/18 staining (Supplementary Fig. S10A). Quantitation of colonic epithelial dextran uptake revealed greater than 10-fold increase in Texas Red fluorescent dextran in the colonic wall of shApc mice as compared with control mice (Fig. 5A and B; Supplementary Fig. S10B), indicating a strong effect of APC knockdown on barrier function.

Increased uptake of dextran by colon cells in shApc mice could be due to activation of macropinocytosis, but could also be due to an increase in colonic wall permeability through disruption of epithelial junctions. Others have demonstrated the early colonic adenomas are characterized by disruption of tight junction and

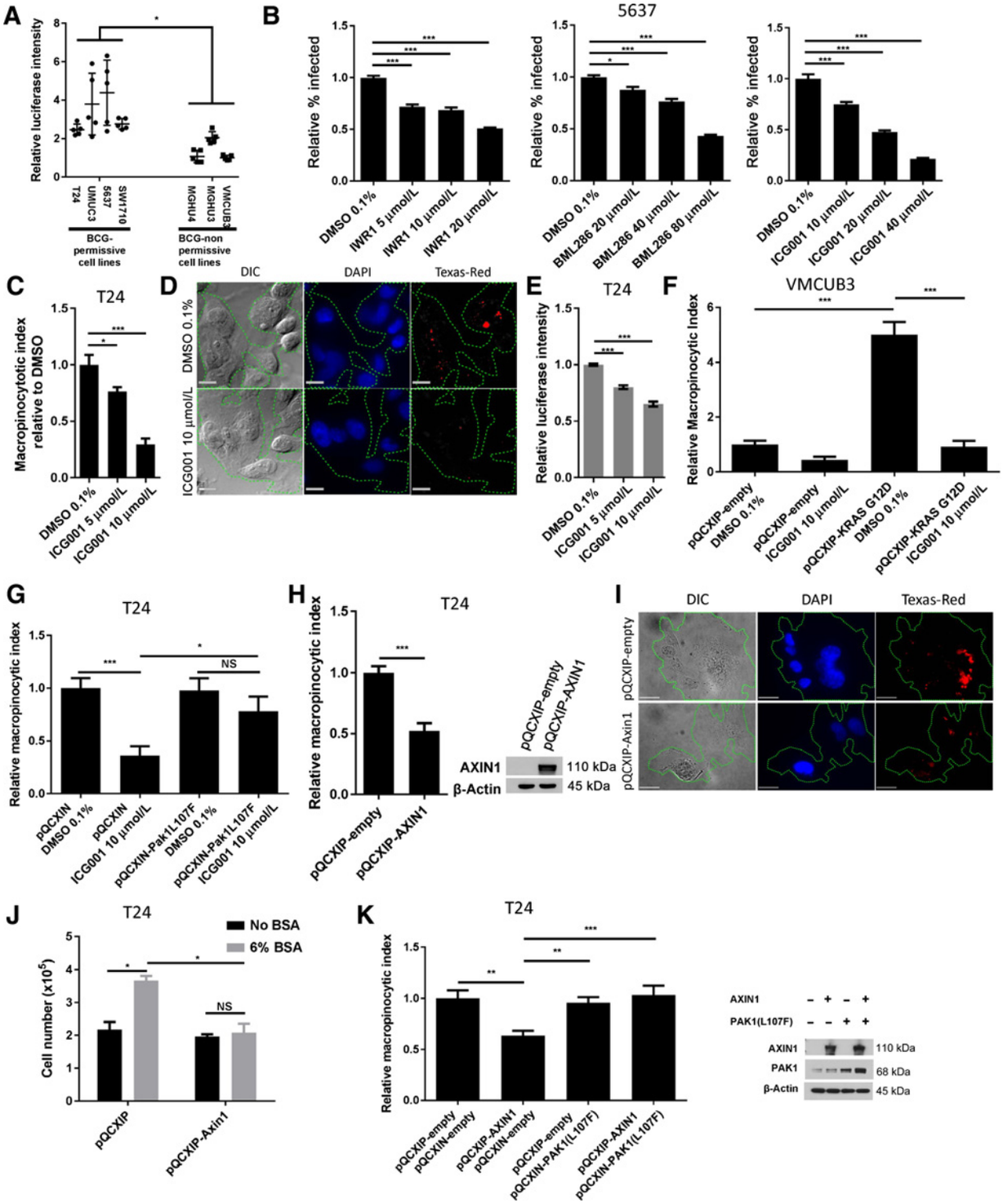

Figure 4.

WNT is an essential cofactor in Ras-driven macropinocytosis **A,** T24, UMUC3, 5637, and SW1710 (permissive for BCG-uptake by macropinocytosis) and MGHU3, MGHU4, and VMCUB3 (nonpermissive for BCG-uptake by macropinocytosis) cells were transduced with the Wnt reporter construct 7TFC. Luciferase expression in cell lysates was measured by luminometry. The data are representative of five independent experiments. Bars, mean ± SEM. **B,** 5637 cells (Ras WT) were incubated with BCG-GFP for 4 hours in the presence of DMSO (vehicle control) or various concentrations of BML286 (disheveled inhibitor), IWR1 (tankyrase inhibitor), or ICG001 (β-catenin-cyclic AMP response element-binding protein inhibitor). Uptake of BCG-GFP was measured by flow cytometry. The data corresponds to the mean of three independent experiments ± SEM. (*Continued on the following page.*)

reduced production of mucin, both of which could increase the permeability of the colonic wall and result in increased uptake of dextran and translocation of bacteria (37). To measure mucin production, we stained colons for MUC2, one of the predominant mucins produced in the gut. We found that shApc colons had a small but significantly decreased MUC2 staining compared with control colons (Fig. 5B; Supplementary Fig. S10C). However, EIPA significantly reversed the elevated dextran uptake resulting from Wnt activation (Fig. 5C and D), indicating that the stimulation of dextran uptake in the colons of shApc mice is due to macropinocytosis and not due to altered epithelial integrity of altered mucin production.

To directly determine whether Wnt activation affects the uptake of intestinal bacteria into the colonic epithelium, we enumerated bacteria within colonic epithelial cells by FISH with a eubacterial 16S ribosomal RNA (rRNA) probe, as described previously (11). We identified nearly 9-fold more bacteria per mm^2 in the colonic wall of shApc mice than in control mice (Fig. 5E and F). Taken together, these results demonstrate that activation of the Wnt pathway in the colon drives colonic macropinocytic uptake of luminal microbiota, the initiating event in colonic tumorigenesis.

Discussion

Using BCG as a probe for macropinocytosis, we find that the canonical Wnt pathway drives PAK1-dependent macropinocytosis and can support tumor cell growth with extracellular protein as a source of essential amino acids. In addition, we show that activation of the Wnt pathway induces macropinocytosis *in vivo* and that this is associated with increased translocation of intraluminal bacteria into the colonic wall.

Our results indicate that the effect of the Wnt pathway on macropinocytosis is mediated through the kinase PAK1. PAK1 is downstream of several pathways, most notably the Ras and *PI3K*–PTEN pathways (41, 42). Several mechanisms of interaction between Ras and the Wnt pathway have been described (43). One means of crosstalk is stabilization of Ras in a manner dependent on glycogen synthase kinase 3β (GSK3β) and the subsequent recruitment of β-TRCP–E3 ligase (44). Our findings, however, suggest that the effect of the Wnt pathway on macropinocytosis is downstream of the Wnt destruction complex and requires nuclear β-catenin. Our findings suggest that transcriptional targets of the Wnt pathway are responsible for activation of macropinocytosis via PAK1, although the identity of these targets remains to be determined. Some potential candidates that have been identified as transcriptional targets of Wnt-dependent transcription factors include *RAB5*, *PDK1*, and *PAK1* itself (45, 46).

Taken most narrowly, our findings may be of relevance for BCG therapy of bladder cancer. We have previously proposed that the efficacy of BCG therapy of bladder cancer depends on uptake of BCG by bladder cancer cells due to the presence of oncogenic aberrations in the Ras and PTEN–*PI3K* pathways, which lead to activation of macropinocytosis (7). Activating mutations in these two pathways are present only in a subset of bladder cancers, however, a substantial fraction of bladder cancers exhibit evidence of Wnt pathway activation (47, 48). Our results suggest that Wnt activation in bladder cancers could promote uptake of BCG and could contribute to their susceptibility to BCG therapy.

More broadly, these findings expand the spectrum of tumor-promoting mutations that stimulate macropinocytosis to fuel tumor growth and may be pertinent to treatment of cancers with activating Ras mutations. Targeting activating mutations of Ras in cancer has been a major challenge. It was proposed that Ras-mutant tumors could be targeted by inhibition of macropinocytosis, thereby starving the cancer of crucial nutrients (3). However, there are no current pharmacologic inhibitors to systemically inhibit macropinocytosis. Our data indicate that inhibition of the Wnt pathway in tumors harboring activating mutations of Ras results in downregulation of macropinocytosis and abrogation of albumin-dependent cell growth. Multiple inhibitors of the Wnt pathway have been developed to date, some of which are currently in clinical trials. Wnt inhibitors might therefore be effective in treating Ras-mutant cancers, even in the absence of detectable Wnt pathway mutational activation.

The earliest stage of oncogenesis in colorectal cancer is Wnt pathway activation, most often due to loss of APC (34, 35). It has been shown that APC loss is sufficient to disrupt the colonic epithelial barrier via decreased production of mucin and aberrant tight junction production with accompanying translocation of bacteria and their products and resulting in IL23/IL17-driven tumor inflammation (37). Several bacterial species, including *Fusobacterium nucleatum* and *Bacteroides fragilis*, have been identified within the epithelial layer in precancerous lesions in patients with familial adenomatous polyposis, as well as in primary and metastatic colorectal tumors, and are thought to directly participate in oncogenesis (49, 50). However, the specific mechanisms that control translocation of bacteria into the epithelial layer were not clear. Our data suggest that APC loss in the colonic epithelium

(*Continued*.) **C,** T24 cells (HRas G12V) were treated with DMSO (vehicle control) or the indicated concentrations of ICG001 for 4 hours, followed by 30 minutes with Texas Red dextran in the presence of DMSO or ICG001. Macropinocytic index was measured. The data correspond to the mean of three independent experiments ± SEM. **D,** Representative images of **C**. Scale bars, 12 μm. Cell borders are outlined in green. **E,** T24 cells were transduced with the Wnt reporter construct 7TFC and incubated with DMSO (vehicle control) or various concentrations of ICG001 for 4 hours. Luciferase expression in cell lysates was measured by luminometry. The data corresponds to the mean of three independent experiments ± SEM. **F,** VMCUB3 cells were transduced with pQCXIP-KRAS(G12D) or with an empty construct. Texas Red dextran was added for 30 minutes and the macropinocytic index was measured. The data correspond to the mean of three independent experiments ± SEM. **G,** T24 cells were with pQCXIN-Pak1(L107F) or with an empty construct. Cells were treated with DMSO (vehicle control) or the indicated concentrations of ICG001 for 4 hours, followed by 30 minutes with Texas Red dextran in the presence of DMSO or ICG001. The macropinocytic index was measured. The data corresponds to the mean of three independent experiments ± SEM. **H,** T24 cells were transduced with pQCXIP-AXIN1 or with an empty construct. Texas Red dextran was added for 30 minutes and the macropinocytic index was measured. Expression of Axin1 was confirmed by Western blot analysis, with β-actin as a loading control. The data correspond to the mean of three independent experiments ± SEM. **I,** Representative images of **H**. Scale bars, 18 μm. Cell borders are outlined in green. **J,** T24 cells were transduced with an pQCXIP-AXIN1 or with an empty construct and grown in leucine-free media for 72 hours in the absence or presence of 6% BSA. At the end of this period, cells were detached and counted. The data correspond to the mean of three independent experiments ± SEM. **K,** T24 cells were transduced with pQCXIP-AXIN1, pQCXIN-PAK1(L107F) or both. Texas Red dextran was added for 30 minutes and the macropinocytic index was measured. Expression of Axin1 and Pak1 was confirmed by Western blot analysis, with β-actin as a loading control. The data correspond to the mean of three independent experiments ± SEM. *P* values for panels **B**, **C**, **E**, **F**, **G**, **J**, and **K** derived by ANOVA with Bonferroni correction. *P* value for **A** and **H** derived by Student *t* test. NS, nonsignificant; DMSO, dimethyl sulfoxide.

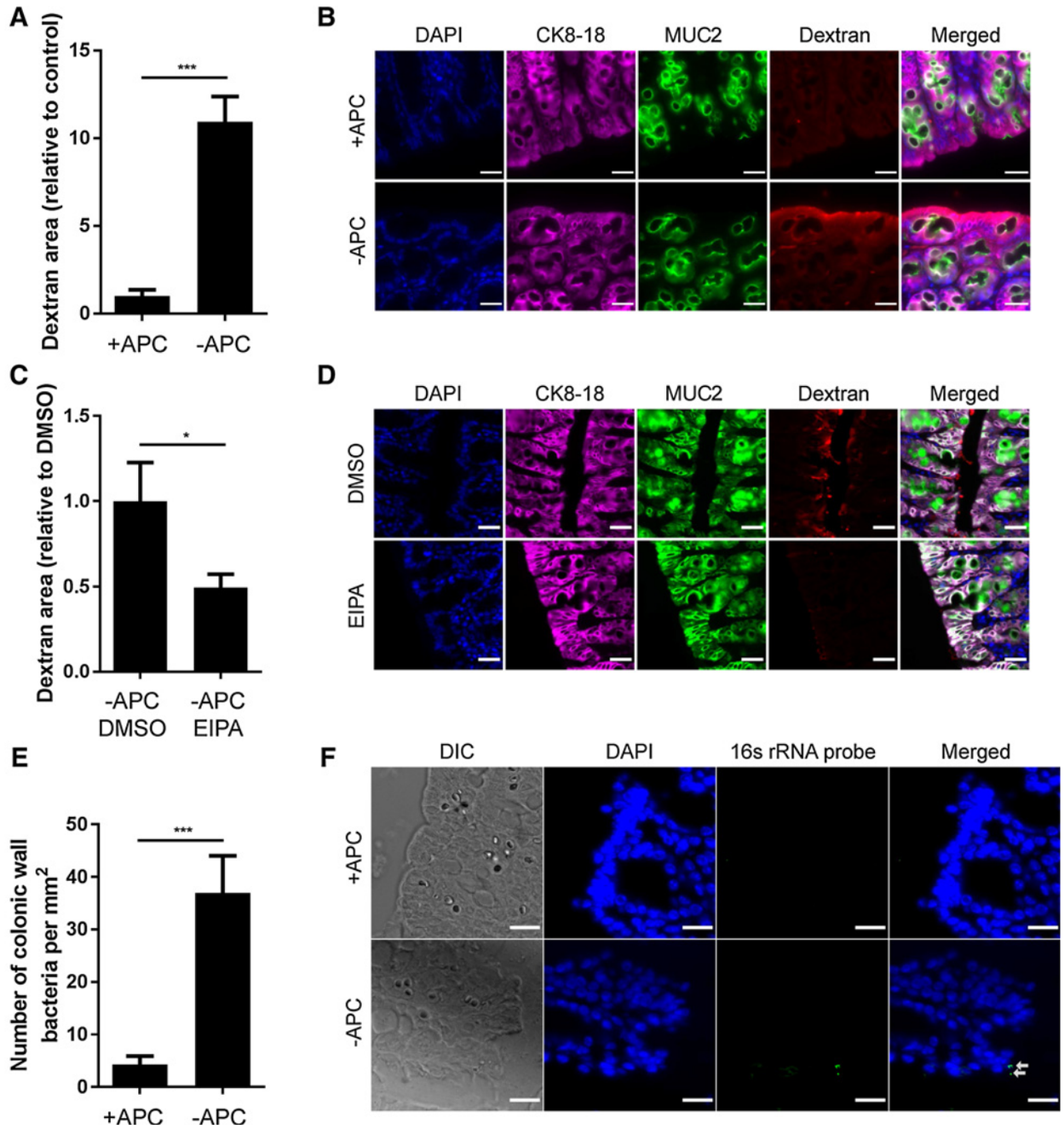

Figure 5.

Wnt pathway activation drives macropinocytic uptake of colonic luminal microbiota. **A,** R26-rtTA TG-Apc.3374 (shApc) mice or R26-rtTA controls were treated with oral doxycycline for 8 days. Mice were anesthetized and Texas Red dextran was instilled into their colons and allowed to dwell for 45 minutes. Colons were removed, fixed, and paraffin-embedded. Sections were stained with antibodies against cytokeratin 8–18 and MUC2. Uptake of dextran was quantified. Results represent four mice per group in two independent experiments. Bars, mean ± SEM. **B,** Representative images of **A**. **C,** R26-rtTA TG-Apc.3374 (shApc) mice or R26-rtTA controls were treated with oral doxycycline for 8 days. Mice were anesthetized and PBS with EIPA or with DMSO (vehicle control) was instilled into their colons. After 30 minutes of incubation, catheters were removed and Texas Red dextran with EIPA or with DMSO was instilled into the colons for an additional 45 minutes. Colons were removed, fixed, and paraffin-embedded. Sections were stained with antibodies against cytokeratin 8–18. Uptake of dextran was quantified. Results represent three mice per group in two independent experiments. Bars represent mean ± SEM. **D,** Representative images of **C**. **E,** R26-rtTA TG-Apc.3374 (shApc) mice or R26-rtTA controls were treated with oral doxycycline for 8 days. Colons were removed, fixed, and paraffin embedded. Sections were stained with a pan-bacterial FISH probe. Uptake of bacteria into the colon wall was quantified by ImageJ as a ratio of number of bacteria in the colon wall to the colon wall area. Results represent three mice per group in two independent experiments. Bars, mean ± SEM. **F,** Representative images of **E**. *P* values derived by ANOVA with Bonferroni correction.

drives macropinocytic bacterial uptake and that this is the critical mediator of increased colonic permeability, rather than altered mucin production or defective tight junctions. The permeability defect is reversed by a topical macropinocytosis inhibitor, both confirming the mechanism of uptake and suggesting a therapeutic strategy for polyposis driven by APC inactivation. These data raise the possibility that Wnt-induced macropinocytosis in early colorectal tumors drives the oncogenic process by contributing to the translocation of luminal microbiota and their products. However, due to the experimental limitations in delivery of EIPA into the colon for extended periods of time, we were unable to directly show an effect of inhibition of Wnt-induced macropinocytosis on tumorigenesis in the colon.

In conclusion, we propose that the Wnt pathway is a previously unappreciated driver of macropinocytosis in cancer.

Disclosure of Potential Conflicts of Interest

No potential conflicts of interest were disclosed.

Authors' Contributions

Conception and design: G. Redelman-Sidi, M.S. Glickman
Development of methodology: G. Redelman-Sidi, W. Palm, C.B. Thompson, S.W. Lowe, M. Bagul, D.E. Root
Acquisition of data (provided animals, acquired and managed patients, provided facilities, etc.): G. Redelman-Sidi, A. Binyamin, I. Gaeta, P.B. Romesser, S.W. Lowe, M. Bagul, J.G. Doench, M.S. Glickman
Analysis and interpretation of data (e.g., statistical analysis, biostatistics, computational analysis): G. Redelman-Sidi, W. Palm, C.B. Thompson, P.B. Romesser, J.G. Doench, M.S. Glickman
Writing, review, and/or revision of the manuscript: G. Redelman-Sidi, I. Gaeta, P.B. Romesser, M.S. Glickman
Administrative, technical, or material support (i.e., reporting or organizing data, constructing databases): A. Binyamin, D.E. Root
Study supervision: M.S. Glickman

Acknowledgments

We thank the members of the MSKCC Molecular Cytology Core Facility for assistance with sample preparation and microscopy. We thank Ralph Garippa for assistance with shRNA design. We acknowledge the following funding sources: NIH P30 CA008748 Cancer Center Support Grant (to G. Redelman-Sidi, A. Binyamin, W. Palm, C.B. Thompson, P.B. Romesser, S.W. Lowe, M.S. Glickman); NIH K08 CA184038 (to G. Redelman-Sidi); NIH R01 CA195787 (to S.W. Lowe); NIH K12 CA184746 (to P.B. Romesser); Starr Cancer Consortium (to M.S. Glickman, D.E. Root). This work was supported by the Starr Cancer Consortium and by the National Cancer Institute at the NIH (K08-CA184038 to G.Redelman-Sidi; K12-CA184746 to P.B. Romesser; RO1-CA195787 to S.W. Lowe; and P30-CA008748)

The costs of publication of this article were defrayed in part by the payment of page charges. This article must therefore be hereby marked *advertisement* in accordance with 18 U.S.C. Section 1734 solely to indicate this fact.

Received October 16, 2017; revised March 5, 2018; accepted June 1, 2018; published first June 5, 2018.

References

1. Swanson JA. Shaping cups into phagosomes and macropinosomes. Nat Rev Mol Cell Biol 2008;9:639–49.
2. Lim JP, Gleeson PA. Macropinocytosis: an endocytic pathway for internalising large gulps. Immunol Cell Biol 2011;89:836–43.
3. Commisso C, Davidson SM, Soydaner-Azeloglu RG, Parker SJ, Kamphorst JJ, Hackett S, et al. Macropinocytosis of protein is an amino acid supply route in Ras-transformed cells. Nature 2013;497:633–7.
4. Kamphorst JJ, Nofal M, Commisso C, Hackett SR, Lu W, Grabocka E, et al. Human pancreatic cancer tumors are nutrient poor and tumor cells actively scavenge extracellular protein. Cancer Res 2015;75:544–53.
5. Palm W, Park Y, Wright K, Pavlova NN, Tuveson DA, Thompson CB. The Utilization of Extracellular Proteins as Nutrients Is Suppressed by mTORC1. Cell 2015;162:259–70.
6. Gontero P, Bohle A, Malmstrom PU, O'Donnell MA, Oderda M, Sylvester R, et al. The role of bacillus Calmette-Guerin in the treatment of non-muscle-invasive bladder cancer. Eur Urol 2010;57:410–29.
7. Redelman-Sidi G, Iyer G, Solit DB, Glickman MS. Oncogenic activation of Pak1-dependent pathway of macropinocytosis determines BCG entry into bladder cancer cells. Cancer Res 2013;73:1156–67.
8. Whittaker SR, Theurillat JP, Van Allen E, Wagle N, Hsiao J, Cowley GS, et al. A genome-scale RNA interference screen implicates NF1 loss in resistance to RAF inhibition. Cancer Discov 2013;3:350–62.
9. Subramanian A, Tamayo P, Mootha VK, Mukherjee S, Ebert BL, Gillette MA, et al. Gene set enrichment analysis: a knowledge-based approach for interpreting genome-wide expression profiles. Proc Natl Acad Sci U S A 2005;102:15545–50.
10. Janakiraman M, Vakiani E, Zeng Z, Pratilas CA, Taylor BS, Chitale D, et al. Genomic and biological characterization of exon 4 KRAS mutations in human cancer. Cancer research 2010;70:5901–11.
11. Caballero S, Carter R, Ke X, Susac B, Leiner IM, Kim GJ, et al. Distinct but Spatially Overlapping Intestinal Niches for Vancomycin-Resistant Enterococcus faecium and Carbapenem-Resistant Klebsiella pneumoniae. PLoS Pathog 2015;11:e1005132.
12. Commisso C, Flinn RJ, Bar-Sagi D. Determining the macropinocytic index of cells through a quantitative image-based assay. Nat Protoc 2014;9:182–92.
13. Fuerer C, Nusse R. Lentiviral vectors to probe and manipulate the Wnt signaling pathway. PLoS One 2010;5:e9370.
14. Yarilin D, Xu K, Turkekul M, Fan N, Romin Y, Fijisawa S, et al. Machine-based method for multiplex in situ molecular characterization of tissues by immunofluorescence detection. Sci Rep 2015;5:9534.
15. Mao B, Niehrs C. Kremen2 modulates Dickkopf2 activity during Wnt/LRP6 signaling. Gene 2003;302:179–83.
16. Mao B, Wu W, Davidson G, Marhold J, Li M, Mechler BM, et al. Kremen proteins are Dickkopf receptors that regulate Wnt/beta-catenin signalling. Nature 2002;417:664–7.
17. Yan D, Wallingford JB, Sun TQ, Nelson AM, Sakanaka C, Reinhard C, et al. Cell autonomous regulation of multiple Dishevelled-dependent pathways by mammalian Nkd. Proc Natl Acad Sci U S A 2001;98:3802–7.
18. Tian X, Du H, Fu X, Li K, Li A, Zhang Y. Smad4 restoration leads to a suppression of Wnt/beta-catenin signaling activity and migration capacity in human colon carcinoma cells. Biochem Biophys Res Commun 2009;380:478–83.
19. Freeman TJ, Smith JJ, Chen X, Washington MK, Roland JT, Means AL, et al. Smad4-mediated signaling inhibits intestinal neoplasia by inhibiting expression of beta-catenin. Gastroenterology 2012;142:562–71 e2.
20. Wu X, Tu X, Joeng KS, Hilton MJ, Williams DA, Long F. Rac1 activation controls nuclear localization of beta-catenin during canonical Wnt signaling. Cell 2008;133:340–53.
21. MacDonald BT, Tamai K, He X. Wnt/beta-catenin signaling: components, mechanisms, and diseases. Dev Cell 2009;17:9–26.
22. Koivusalo M, Welch C, Hayashi H, Scott CC, Kim M, Alexander T, et al. Amiloride inhibits macropinocytosis by lowering submembranous pH and preventing Rac1 and Cdc42 signaling. J Cell Biol 2010;188:547–63.
23. Deacon SW, Beeser A, Fukui JA, Rennefahrt UE, Myers C, Chernoff J, et al. An isoform-selective, small-molecule inhibitor targets the autoregulatory mechanism of p21-activated kinase. Chem Biol 2008;15:322–31.
24. Komiya Y, Habas R. Wnt signal transduction pathways. Organogenesis 2008;4:68–75.
25. Niehrs C. Function and biological roles of the Dickkopf family of Wnt modulators. Oncogene 2006;25:7469–81.
26. Lee AY, He B, You L, Xu Z, Mazieres J, Reguart N, et al. Dickkopf-1 antagonizes Wnt signaling independent of beta-catenin in human mesothelioma. Biochem Biophys Res Commun 2004;323:1246–50.

27. Emami KH, Nguyen C, Ma H, Kim DH, Jeong KW, Eguchi M, et al. A small molecule inhibitor of beta-catenin/CREB-binding protein transcription [corrected]. Proc Natl Acad Sci U S A 2004;101:12682–7.
28. Miyoshi Y, Ando H, Nagase H, Nishisho I, Horii A, Miki Y, et al. Germ-line mutations of the APC gene in 53 familial adenomatous polyposis patients. Proc Natl Acad Sci U S A 1992;89:4452–6.
29. Tsujimura N, Yamada NO, Kuranaga Y, Kumazaki M, Shinohara H, Taniguchi K, et al. A Novel Role of Dickkopf-Related Protein 3 in Macropinocytosis in Human Bladder Cancer T24 Cells. Int J Mol Sci 2016;17.
30. Nakamura T, Hamada F, Ishidate T, Anai K, Kawahara K, Toyoshima K, et al. Axin, an inhibitor of the Wnt signalling pathway, interacts with beta-catenin, GSK-3beta and APC and reduces the beta-catenin level. Genes Cells 1998;3:395–403.
31. Palm W, Thompson CB. Nutrient acquisition strategies of mammalian cells. Nature 2017;546:234–42.
32. Grandy D, Shan J, Zhang X, Rao S, Akunuru S, Li H, et al. Discovery and characterization of a small molecule inhibitor of the PDZ domain of dishevelled. J Biol Chem 2009;284:16256–63.
33. Narwal M, Venkannagari H, Lehtio L. Structural basis of selective inhibition of human tankyrases. J Med Chem 2012;55:1360–7.
34. Thorstensen L, Lind GE, Lovig T, Diep CB, Meling GI, Rognum TO, et al. Genetic and epigenetic changes of components affecting the WNT pathway in colorectal carcinomas stratified by microsatellite instability. Neoplasia 2005;7:99–108.
35. Groden J, Thliveris A, Samowitz W, Carlson M, Gelbert L, Albertsen H, et al. Identification and characterization of the familial adenomatous polyposis coli gene. Cell 1991;66:589–600.
36. Li Y, Kundu P, Seow SW, de Matos CT, Aronsson L, Chin KC, et al. Gut microbiota accelerate tumor growth via c-jun and STAT3 phosphorylation in APCMin/+ mice. Carcinogenesis 2012;33:1231–8.
37. Grivennikov SI, Wang K, Mucida D, Stewart CA, Schnabl B, Jauch D, et al. Adenoma-linked barrier defects and microbial products drive IL-23/IL-17-mediated tumour growth. Nature 2012;491:254–8.
38. Kostic AD, Chun E, Robertson L, Glickman JN, Gallini CA, Michaud M, et al. Fusobacterium nucleatum potentiates intestinal tumorigenesis and modulates the tumor-immune microenvironment. Cell Host Microbe 2013;14:207–15.
39. Premsrirut PK, Dow LE, Kim SY, Camiolo M, Malone CD, Miething C, et al. A rapid and scalable system for studying gene function in mice using conditional RNA interference. Cell 2011;145:145–58.
40. Dow LE, O'Rourke KP, Simon J, Tschaharganeh DF, van Es JH, Clevers H, et al. Apc Restoration promotes cellular differentiation and reestablishes crypt homeostasis in colorectal cancer. Cell 2015;161:1539–52.
41. Lambert JM, Lambert QT, Reuther GW, Malliri A, Siderovski DP, Sondek J, et al. Tiam1 mediates Ras activation of Rac by a PI(3)K-independent mechanism. Nat Cell Biol 2002;4:621–5.
42. Kumar R, Gururaj AE, Barnes CJ. p21-activated kinases in cancer. Nat Rev Cancer 2006;6:459–71.
43. Zeller E, Hammer K, Kirschnick M, Braeuning A. Mechanisms of RAS/beta-catenin interactions. Arch Toxicol 2013;87:611–32.
44. Jeong WJ, Yoon J, Park JC, Lee SH, Lee SH, Kaduwal S, et al. Ras stabilization through aberrant activation of Wnt/beta-catenin signaling promotes intestinal tumorigenesis. Sci Signal 2012;5:ra30.
45. Lanzetti L, Palamidessi A, Areces L, Scita G, Di Fiore PP. Rab5 is a signalling GTPase involved in actin remodelling by receptor tyrosine kinases. Nature 2004;429:309–14.
46. Pate KT, Stringari C, Sprowl-Tanio S, Wang K, TeSlaa T, Hoverter NP, et al. Wnt signaling directs a metabolic program of glycolysis and angiogenesis in colon cancer. EMBO J 2014;33:1454–73.
47. Schmid SC, Sathe A, Guerth F, Seitz AK, Heck MM, Maurer T, et al. Wntless promotes bladder cancer growth and acts synergistically as a molecular target in combination with cisplatin. Urol Oncol 2017.
48. Costa VL, Henrique R, Ribeiro FR, Carvalho JR, Oliveira J, Lobo F, et al. Epigenetic regulation of Wnt signaling pathway in urological cancer. Epigenetics 2010;5:343–51.
49. Bullman S, Pedamallu CS, Sicinska E, Clancy TE, Zhang X, Cai D, et al. Analysis of Fusobacterium persistence and antibiotic response in colorectal cancer. Science 2017;358:1443–8.
50. Dejea CM, Fathi P, Craig JM, Boleij A, Taddese R, Geis AL, et al. Patients with familial adenomatous polyposis harbor colonic biofilms containing tumorigenic bacteria. Science 2018;359:592–7.